

Estimate of three-dimensional flexural-isostatic response to unloading: Rock uplift due to late Cenozoic glacial erosion in the western United States

Jon D. Pelletier* Department of Geosciences, University of Arizona, Gould-Simpson Building, 1040 East Fourth Street, Tucson, Arizona 85721-0077, USA

ABSTRACT

Alpine glacial erosion may strongly influence mountain building through erosionally driven rock uplift and relief production. In this paper I use a three-dimensional model for the flexural-isostatic response of the lithosphere to estimate the potential for late Cenozoic erosionally driven rock uplift in the western United States. Specifically, I present a map of the ratio of erosionally driven rock uplift to glacial erosion for this region. This ratio depends on the magnitude of the flexural bending stresses that act to limit differential uplift. The map is created by constraining the extent of Pliocene–Quaternary alpine glacial erosion in the western United States and solving the three-dimensional flexure equation for the resulting lithospheric deflection. The map indicates that the magnitude of erosionally driven uplift depends sensitively on the size of the glaciated range and the presence of nearby glaciated ranges. As a result, regional-scale patterns must be considered in order to correctly estimate local amounts of erosionally driven rock uplift. The ranges in the western United States with the greatest ratios of uplift to erosion are the San Juan Mountains and the Yellowstone Plateau–Absaroka Range, because these are extensively glaciated and have glaciated ranges nearby. In contrast, the Wind River Range and Sierra Nevada have ratios of uplift to erosion that are only half as large. These results identify which ranges likely underwent the greatest erosionally driven uplift and relief production and provide a widely applicable technique for modeling the flexural-isostatic response to loading and unloading in three dimensions.

Keywords: uplift, isostasy, late Cenozoic, glaciation.

INTRODUCTION AND BACKGROUND

Molnar and England (1990) suggested that evidence for late Cenozoic tectonic uplift in many areas worldwide could instead be the result of relief production driven by enhanced fluvial or glacial erosion resulting from global cooling. This hypothesis touched off a vigorous debate on the ability of erosion to enhance relief. Although fluvial erosion has generally been regarded as insufficiently focused in the landscape to enhance relief (Montgomery, 1994; Whipple et al., 1999), alpine-glacial erosion may be more effective because it is concentrated in valleys and near the equilibrium line. Farley et al. (2001) argued in favor of the ability of glacial erosion to enhance relief by suggesting that most of the relief of the British Columbia Coast Mountains was produced by erosionally driven rock uplift in the past 2.5 m.y. Similarly, Hay et al. (2003) attributed 800 m of late Cenozoic peak uplift in the Alps to erosionally driven uplift. In the Sierra Nevada and Wind River Range, Small and Anderson (1995, 1998) calculated relief production of several hundred meters—modest but significant amounts. Whipple et al. (1999), however, argued that glacial relief pro-

duction was likely limited to a few hundred meters at most anywhere in the world. It is difficult to be definitive about the magnitude of erosionally driven rock uplift and relief production because the processes are difficult to quantify. For example, of all of these studies, Small and Anderson (1995, 1998) quantified the processes of erosion and uplift most carefully, but their analysis was still limited to a two-dimensional geometry that assumed uniform elastic thickness and did not consider the effects of erosion in nearby ranges.

A complete assessment of the role of glacial erosion in rock uplift and relief production will require new results in thermochronology, cosmogenic erosion-rate measurements, and three-dimensional numerical landform-evolution modeling. As a step toward this goal, this paper provides a widely applicable numerical method for calculating the rock uplift resulting from erosion either in a numerical model or in the real world. As the geomorphic and tectonics communities strive to develop accurate three-dimensional numerical models for investigating feedbacks among erosion, climate, and uplift, the flexural-isostatic response to erosion must be precisely determined. The method of this paper uses two types of

input—elastic thickness data and the spatial distribution of erosion—to predict the spatial pattern of rock uplift, taking into account spatial variations in elastic strength. Here I illustrate the method by evaluating the ratio of late Cenozoic erosionally driven rock uplift to glacial erosion in the western United States. Areas where this ratio is large have likely undergone the greatest relief production and should be the focus of future efforts to identify signatures of erosionally driven rock uplift and relief production.

The ratio of erosionally driven rock uplift to erosion depends on the area and shape of the eroded region and on the local flexural wavelength of the lithosphere. If the flexural wavelength is large compared with the width of the glaciated region, uplift will be limited by flexural bending stresses. In contrast, if the flexural wavelength and the width of the eroded region are comparable, bending stresses will be smaller and uplift will approach the Airy isostatic limit, in which 80% of the eroded material is replaced through rock uplift. The concept of a ratio of erosionally driven uplift to erosion is similar to the “degree of compensation” of the lithosphere under a periodic load; I refer to this ratio as a compensation that is defined between 0 and 1. However, compensation as defined here does not assume periodic loading—the actual load is considered.

To map the compensation resulting from glacial erosion, I first determined the spatial distribution of glaciated regions in the western United States. Second, I solved the three-dimensional flexural equation with variable elastic thickness to determine the deflection of the lithosphere in response to erosional unloading. In my analyses I assumed two different hypotheses for the distribution of glacial erosion within the glaciated area: erosion that was (1) uniform within the glaciated region or (2) concentrated near the elevation of the lowest cirques (herein referred to as the “glacial limit”). Assuming uniform erosion results in slightly higher compensation values, but the results are not significantly different. My analysis shows that in all the major ranges of the western United States, compensation reaches maximum values of 0.4 or greater; this result indicates that significant erosionally driven

*E-mail: jon@geo.arizona.edu.

uplift has occurred in the region during the late Cenozoic, if it can be assumed that glacial erosion was also significant. Some areas of extensive glaciation have compensation values to three times higher than other ranges. For example, compensation in the Sierra Nevada and Wind River Range is modest in comparison to compensation in the Yellowstone Plateau–Absaroka Range and San Juan Mountains. As a result, relief production in the Yellowstone Plateau–Absaroka Range and San Juan Mountains may have been significantly greater than the several hundred meters previously calculated by Small and Anderson (1995, 1998) for the Sierra Nevada and Wind River Range, where flexural bending stresses were a limiting factor in isostatic uplift and relief production.

DISTRIBUTION OF LATE CENOZOIC GLACIAL EROSION IN THE WESTERN UNITED STATES

Porter et al. (1983) mapped areas of Pliocene–Quaternary glaciation in the western United States, based on the elevations of the lowest cirques. Their map identifies the approximate local elevation of vigorous glacial erosion. To construct a map of the extent of late Cenozoic glacial erosion, I first digitized the contours of glacial-limit elevation from Porter et al. (1983), projected them to Lambert equal area, and interpolated the contours to obtain a grid of glacial-limit elevations. Second, a 1-km-resolution digital elevation model (DEM) of the western United States was rectified to the glacial-limit-elevation grid. Third, the glacial-limit-elevation and DEM grids were compared pixel by pixel to determine whether local elevations were above or below the glacial-limit elevation. Pixels with elevations above the glacial limit were considered areas of glacial erosion and were given a value of 1. Conversely, pixels with elevations below the glacial limit were considered not to have been subjected to glacial erosion and were given a value of 0. The resulting binary grid is a map of relative glacial erosion; an underlying assumption is that erosion is uniform within the glaciated regions. The boundaries of the glaciated regions obtained in this way are mapped in white in Figure 1 (which also shows state boundaries for reference). Also shown in Figure 1 is a gray-scale map of the elastic thickness in the western United States (discussed in the following section). Ranges along the Pacific coast were not included in Porter et al. (1983) and have also been excluded from my analysis. In addition, the northern Cascades were excluded because they were completely covered by the Cordilleran Ice Sheet and hence subject to a different style of glaciation than other ranges of the

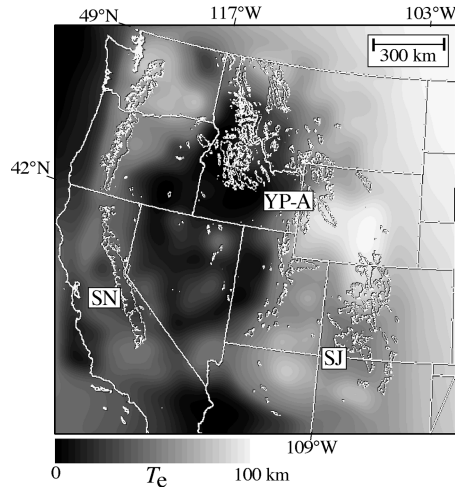


Figure 1. Gray-scale map of elastic thickness (T_e) in western United States. Data are from Lowry et al. (2000) and Watts (2001). Boundaries of glaciated areas are shown in white. Labeled ranges: SN (Sierra Nevada), SJ (San Juan), and YP-A (Yellowstone Plateau–Absaroka).

western United States. The resulting map of glacial extent says nothing about the magnitude of glacial erosion. However, the magnitude of glacial erosion is not needed to determine the ratio of erosionally driven rock uplift to erosion—only the relative distribution of erosion is required. Although this method of reconstructing glacial extents is an effective means of digitally mapping glaciation over a large region, it is of limited accuracy in reproducing the fine details of glaciation within each range. This is not a significant limitation, however, because compensation values are insensitive to small-scale spatial variations in erosion.

As an alternative erosion distribution, I constructed a second binary grid that assumes that erosion is concentrated close to the glacial limit. To construct this grid, I assigned values of 1 to pixels with elevations between the glacial-limit elevation and 500 m above the glacial-limit elevation. All other pixels were assumed to have undergone no erosion and were given a value of 0. The 500 m range is arbitrary, but was chosen so that the cores of most western United States ranges were designated as areas of no erosion. These two hypotheses represent simple idealizations of the spatial distributions of erosion. It is likely that these distributions are underestimates, because fluvial erosion below the glacial limit is not considered. It is important to note, however, that the compensation maps obtained by using these different assumptions are very similar.

A key assumption in my analysis is that most of the material eroded from the mountains is carried far from the source (relative to the flexural wavelength) over late Cenozoic

time scales. This is an important assumption because eroded material that is stored close to the source will not contribute to erosional unloading. Evidence for efficient sediment evacuation comes from the modest thickness of late Cenozoic sediment in several western United States basins. Pliocene–Quaternary sediments in the San Luis Valley adjacent to the San Juan Mountains, for example, are generally 15–55 m thick (Huntley, 1979). Similarly, late Cenozoic sediments in the Denver basin are between 0 and 140 m thick (Baars et al., 1988). The Bighorn and Powder River Basins have undergone net erosion during the late Cenozoic as a result of isostatic uplift, transporting most of the Pliocene–Quaternary sediment through the basin in addition to significant amounts of older sediments (Love, 1960). If, however, late Cenozoic sediments are thick near the source, my analysis provides an upper bound for compensation.

COMPENSATION MAPPING BY SOLUTION OF THE FLEXURE EQUATION

The deflection of a thin elastic plate with variable elastic thickness under a vertical load is given by

$$\nabla^2[D(x, y)\nabla^2w] + \Delta\rho gw = q(x, y), \quad (1)$$

where w is the deflection, $D(x, y)$ is the flexural rigidity, $\Delta\rho$ is the density contrast between the crust and the mantle, g is acceleration due to gravity, and $q(x, y)$ is the vertical load (Watts, 2001). Elastic stresses are responsible for the harmonic (∇^2) terms, and buoyancy forces induced by the displacement of high-density mantle with lower-density crust are responsible for the linear term. If spatial variations in elastic thickness are accounted for, as in equation 1, then $D(x, y)$ must remain inside the brackets; the result is additional terms involving gradients of D that are not present in the more commonly assumed case of uniform elastic thickness.

The binary grids of glacial erosion that I constructed were directly input into the flexure equation as the loading term, so that $q(x, y) = 1$ where erosion occurred and $q(x, y) = 0$ where erosion did not occur. The solution to the flexure equation with these loading terms is the ratio of the positive deflection of the lithosphere to the depth of glacial erosion. This is the compensation resulting from glacial erosion. I used the alternating difference implicit (ADI) technique to solve equation 1, following the work of van Wees and Cloetingh (1994). A direct approach to solving equation 1 would be to frame it as a matrix equation for the values of $w(x, y)$ at each point on the grid. This approach, however, would require inverting a matrix with $L^2 \times W^2$ elements

(where L and W are the length and width of the grid in pixels), which is impossible for all but the smallest grids. ADI works by reducing the solution of equation 1 to an iterative sequence of two-dimensional matrix equations. Two-dimensional problems have two advantages. First, they require the inversion of much smaller matrices. Second, the required matrices have a pentadiagonal form in the case of fourth-order partial differential equations (such as equation 1), which are inverted much more rapidly than the general matrices of the three-dimensional case. To reduce the three-dimensional problem to two dimensional, a solution is obtained for the deflection in each row and column successively during each iteration, by using the bending stresses in the orthogonal direction as part of the loading term. This procedure converges to the exact solution.

For my analysis, I used Lowry et al.'s (2000) data set for elastic thickness (T_e) in the western United States. These data are based on the coherence method and provide a direct measure of lithospheric strength that includes the weakening effects of faults. These data have the highest resolution available for the region, but do not completely cover the western United States. To cover the entire area, I augmented the Lowry et al. data with the global compilation of Watts (2001), joining the data sets smoothly with a low-pass filter. The resulting T_e map was rectified to the glacial erosion maps and is shown as a gray-scale map in Figure 1. The T_e values were converted to a grid of flexural rigidity, $D(x, y)$, for use in equation 1, by means of $D = ET_e^3/[12(1 - \nu^2)]$ and by assuming $E = 70$ GPa and $\nu = 0.25$. This procedure produces the most accurate constraints on elastic thickness for the western United States. However, nearly identical results were obtained by using the Watts (2001) data alone, suggesting that compensation values do not depend sensitively on small-scale variations in elastic thickness. As such, the Watts compilation could be used with available DEMs to provide estimates of compensation anywhere in the world where glacial-limit elevations can be estimated.

COMPENSATION OF GLACIAL EROSION IN THE WESTERN UNITED STATES

Color maps of the compensation in the western United States are given for the cases of uniform erosion (Fig. 2A) and erosion concentrated near the glacial limit (Fig. 2B). Although compensation is strictly defined to be between 0 and 1, I have mapped the full solution to the flexure equation in Figure 2, including areas of minor subsidence (in black). All of the major ranges in the western United

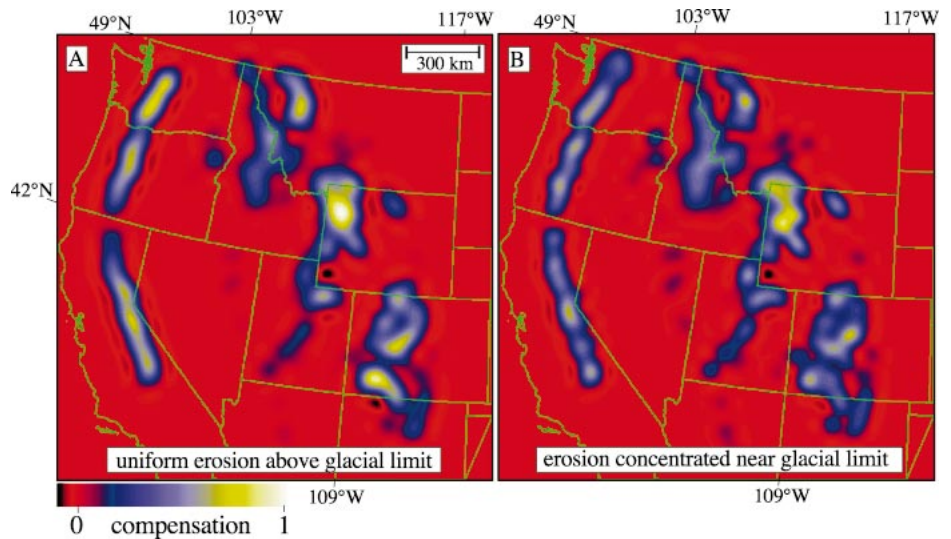


Figure 2. Color map of compensation of glacial erosion assuming (A) uniform erosion within glaciated areas and (B) erosion concentrated within 500 m altitude of glacial limit.

States have compensation values ≥ 0.4 , indicating that nearly half of all glacially eroded mass is returned to the region's ranges as erosionally driven rock uplift. The pattern of compensation varies little between Figures 2A and 2B because flexure is insensitive to small-scale variations in loading. The greatest difference between Figures 2A and 2B is the mean values: values of compensation obtained by assuming concentrated erosion near the glacial limit are $\sim 20\%$ lower than for uniform erosion. These lower values reflect the additional bending stresses present in the case of

localized erosion; i.e., for the same eroded mass, a circular area (i.e., uniform erosion within the range) results in less intense bending stresses than a ring-shaped area (i.e., localized erosion near the glacial limit).

The two areas of highest compensation in the western United States are the Yellowstone Plateau–Absaroka Range and the San Juan Mountains. Under the assumption of uniform erosion (Fig. 2A), the Yellowstone Plateau–Absaroka Range achieves compensation values between 0.8 and 1.0 in the central 100 km of the region. The San Juan Mountains reach

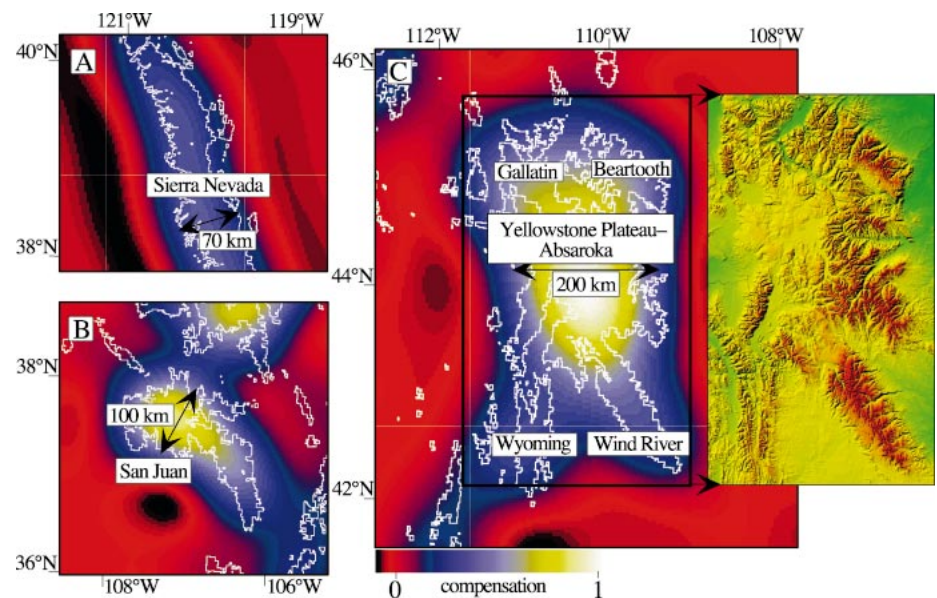


Figure 3. Regional examples of variations in compensation. A: Central Sierra Nevada has glaciated width of 70 km and maximum compensation of 0.4. B: San Juan Mountains have glaciated width of ~ 100 km at their narrowest point and have maximum compensation of 0.9. C: Greatest compensation values in western United States are found in Yellowstone Plateau–Absaroka Range, which is both extensive (~ 200 km in width) and surrounded by four other glaciated ranges. Locations are shown in Figure 1. Geographic bounds are approximate due to map projection.

a maximum value of 0.9. The high compensation of the San Juan Mountains illustrates an important control on compensation: it is very sensitive to the width of the glaciated region. A comparison of the glaciated extents and compensation values of the San Juan and Sierra Nevada ranges, shown in Figures 3A and 3B, helps to illustrate this point. Both ranges are approximately isolated (the Sierra Nevada has no glaciated ranges within 500 km to the east or west, whereas the San Juan Mountains are only slightly affected by the glacial erosion of the Rocky Mountains), so they can be considered without including the glaciation of nearby ranges. The width of Sierran glaciation is ~70 km, whereas the width of the San Juan glaciation, although more irregular in shape, is ~100 km at its narrowest point. Even this 30% difference in the width of two glaciated regions can result in a doubling of compensation values. Compensation values are sensitive to the width of the glaciated range because flexural bending stresses are proportional to the fourth power of the wavelength of the glaciated region. The sensitivity of compensation to small changes in the width of the glaciated area suggests that care must be taken to include all regional erosion when estimating erosionally driven rock uplift, including areas to several hundred kilometers away from the area of interest. For this reason, it may be necessary to revise previously published estimates for isostatic uplift. For example, Small and Anderson performed a classic study of relief production in the Wind River Range; however, they estimated glacial erosion only within the central core of the range where summit flats are preserved (~30 km in width), even though the glaciated area of the Wind River Range is ~50 km in width. As such, their estimate is probably a lower limit.

The highest compensation values in the western United States are found in the Yellowstone Plateau–Absaroka Range. The high values in this region reflect the extensiveness of the glaciated area, which is nearly 200 km in width (Fig. 3C). In addition, however, nearby ranges are also being eroded, reducing the bending stresses that would otherwise be concentrated at the edges of the Yellowstone area, limiting its potential uplift. Instead, nearby ranges, including the Beartooth, Gallatin, Wyoming, and Wind River Ranges, accommodate the bending stresses to produce a “bulls-eye” over the central part of the area—the Yellowstone Plateau–Absaroka Range. Although Figure 3 suggests that the width of the glaciated

region is the only control on compensation, the elastic thickness also plays a role if it varies significantly over the region. However, the elastic thicknesses of the Sierra Nevada, San Juan Mountains, and Yellowstone area are similar enough that glaciated area is the most significant controlling variable.

SUMMARY AND CONCLUSIONS

A realistic three-dimensional model of the flexural-isostatic response of the lithosphere will be an essential component of any state-of-the-art tectonic landform-evolution model. This paper describes a simple numerical method that provides this key component. The method, when applied to estimating the compensation to glacial erosion in the western United States, indicates that regional-scale erosion must be considered in order to accurately estimate erosionally driven uplift and relief production. Moreover, there is significant spatial variability in compensation; the San Juan and Yellowstone areas are the most likely regions to have undergone significant rock uplift and relief production.

A complete answer to the role of glacial erosion in mountain building will require that small-scale spatial variations in erosion be resolved and that glacial erosion rates be better constrained. Although this is a daunting task, three important techniques are available that will greatly improve our knowledge. First, low-temperature thermochronology (e.g., House et al., 2001) will provide constraints on paleorelief that can enable a direct assessment of relief production. Second, numerical modeling of alpine glacial erosion (e.g., Tomkin and Braun, 2002) will provide information on the spatial variability of erosion and the feedbacks between glacial erosion, topography, and glacier morphology. Finally, sediment fluxes in modern glacial systems (e.g., Hallet et al., 1996) will provide a guide for estimating mean glacial erosion rates. Together with the information provided by these important techniques, the methodology of this paper will improve our understanding of the role of glaciation in mountain building.

ACKNOWLEDGMENTS

I thank Tony Watts and Tony Lowry for providing their elastic thickness data and two anonymous reviewers for their help in improving the paper.

REFERENCES CITED

Baars, D.L., and 15 others, 1988, Basins of the Rocky Mountain region, in Sloss, L.L., ed., *Sedimentary cover—North American craton*; U.S.: Boulder, Colorado Geological Society of America, *Geology of North America*, v. D-2, p. 109–220.

- Farley, K.A., Rusmore, M.E., and Bogue, S.W., 2001, Post-10 Ma uplift and exhumation of the northern Coast Mountains, British Columbia: *Geology*, v. 29, p. 99–102.
- Hallet, B., Hunter, L., and Bogen, J., 1996, Rates of erosion and sediment evacuation by glaciers: A review of field data and their implications: *Global and Planetary Change*, v. 12, p. 213–235.
- Hay, W.W., Soeding, E., DeConto, R.M., and Wold, C.N., 2003, The late Cenozoic uplift—Climate change paradox: *International Journal of Earth Sciences*, v. 91, p. 746–774.
- House, M.A., Wernicke, B.P., and Farley, K.A., 2001, Paleo-geomorphology of the Sierra Nevada, California, from (U-Th)/He ages in apatite: *American Journal of Science*, v. 301, p. 77–102.
- Huntley, D., 1979, Cenozoic faulting and sedimentation in northern San Luis Valley, Colorado: Summary: *Geological Society of America Bulletin*, v. 90, p. 8–10.
- Love, J.D., 1960, Cenozoic sedimentation and crustal movements in Wyoming: *American Journal of Science*, v. 258-A, p. 204–214.
- Lowry, A.R., Ribe, N.M., and Smith, R.B., 2000, Dynamic elevation of the Cordillera, western United States: *Journal of Geophysical Research*, v. 105, p. 23,371–23,390.
- Molnar, P., and England, P., 1990, Late Cenozoic uplift of mountain ranges and global climate changes: Chicken or egg?: *Nature*, v. 346, p. 29–34.
- Montgomery, D.R., 1994, Valley incision and the uplift of mountain peaks: *Journal of Geophysical Research*, v. 99, p. 13,913–13,921.
- Porter, S.C., Pierce, K.L., and Hamilton, T.D., 1983, Late Wisconsin mountain glaciation in the western United States, in Wright, H.E., Jr., and Porter, S.C., eds., *Late Quaternary environments of the United States, Volume 1: Minneapolis*, University of Minnesota Press, p. 71–115.
- Small, E.E., and Anderson, R.S., 1995, Geomorphically driven late Cenozoic rock uplift in the Sierra Nevada, CA: *Science*, v. 270, p. 277–280.
- Small, E.E., and Anderson, R.S., 1998, Pleistocene relief production in Laramide mountain ranges, western United States: *Geology*, v. 26, p. 123–126.
- Tomkin, J.H., and Braun, J., 2002, The influence of alpine glaciation on the relief of tectonically active mountain belts: *American Journal of Science*, v. 302, p. 169–190.
- van Wees, J.D., and Cloetingh, S., 1994, A finite-difference technique to incorporate spatial variations in rigidity and planar faults into 3-D models for lithospheric flexure: *Geophysical Journal International*, v. 117, p. 179–195.
- Watts, A.B., 2001, *Isostasy and flexure of the lithosphere*: Cambridge, Cambridge University Press, 458 p.
- Whipple, K.X., Kirby, E., and Brocklehurst, S.H., 1999, Geomorphic limits to climate-induced increases in topographic relief: *Nature*, v. 401, p. 39–43.

Manuscript received 29 July 2003

Revised manuscript received 16 October 2003

Manuscript accepted 20 October 2003

Printed in USA